

# Field emission theory beyond WKB - the full image problem

T C Choy, A H Harker and A M Stoneham

Department of Physics and Astronomy, University College London, Gower Street,  
London WC1E 6BT

E-mail: a.harker@ucl.ac.uk

**Abstract.** The classic theory of electron field emission from a cold metal surface due to Fowler and Nordheim (FN) is re-examined and found to violate the validity criteria for the WKB approximation, for electric fields greater than about  $1 \text{ V}/\mu\text{m}$ . In this study we shall examine the complete solution without invoking the WKB approximation in order to assess the reliability of the FN theory as widely used for the interpretation of experimental data. Particular problems occur when the barrier height (and therefore indirectly also the width) is significantly reduced by the image or some external effects. Further refinement of the theory will be discussed by considering the effects of screening, which can be one mechanism for the barrier height reduction, in addition to the widely known negative affinity of diamond like carbon systems. A comparison with experimental data from carbon field emitters shows that the enhanced current found in this paper may provide an explanation for strong field emission observed recently in carbon based samples.

Submitted to: *JPCM*

PACS numbers: 72.20.-i,72.20.Fr,72.20.Ht,73.40.-c

## Introduction

The classic theory of electron field emission from a cold metal surface due to Fowler and Nordheim (FN) [1, 2, 3] was one of the earliest applications of wave mechanics since its foundation in the early 1920's. With increased interest in field emission processes, especially for use in display screens [4], it is worth examining closely the foundations of this theory. As well as metal-vacuum interfaces, proposed applications of the theory includes graphite-vacuum, graphite-insulator-vacuum, carbon-nanotube-vacuum and Schottky junctions [5]. Since our approach can be generalized to other cases of interfaces between dissimilar media, it may have application to the systems discussed by Mott and Gurney [6] and Herring [7]. These other cases might include vacuum breakdown and electrical forming processes [8]. In section 5 we show that our new analysis removes discrepancies of many orders of magnitude between theory and experiment.

In the FN theory, the role of the Fermi surface, Fermi-Dirac statistics and in particular the unique property of quantum mechanical tunnelling were key concepts. The essentially equilibrium distribution of electrons is modeled by a one dimensional ( $x$  dependent only) Hamiltonian:

$$H_0 = \frac{p_x^2}{2m} + V(x), \quad (1)$$

where all energies are measured with the same reference as the effective potential  $V(x)$ . Then the current density  $J$  of the emitted electrons is given by an integral over the energy  $W$ :

$$J = e \int_{-W_a}^{\infty} P(W) dW, \quad (2)$$

where  $P(W)dW$  gives the number of electrons within  $dW$  that emerge from the metal per second per unit area, with  $W_a$  an appropriate lower energy reference. The quantity  $P(W)$  is easily expressed as the product of a quantum mechanical tunnelling transmission coefficient  $T(W)$  and a Fermi type supply function  $N(W)$ :

$$N(W) = \frac{4\pi mkT}{h^3} \ln \left\{ 1 + \exp \left[ -\left( \frac{W - \epsilon_F}{kT} \right) \right] \right\}, \quad (3)$$

in which  $\epsilon_F$  is the Fermi energy. In view of the complexity of the Schrodinger equation, the transmission problem was originally treated within a WKB approximation or variants of it [9]:

$$T(W) = \exp \left[ - \int_{x_1}^{x_2} \left( \frac{8m}{\hbar^2} (V(x) - W) \right)^{1/2} dx \right], \quad (4)$$

in which  $x_1$  and  $x_2$  are the classical turning points of the potential  $V(x)$ . It is a well known result however that the validity of the WKB approximation involves a criterion, see section 1, that can be derived from the requirement that the variation of the deBroglie wavelength of the electron must be less than the dimension of the region of tunnelling [10]. This restriction on the validity of the FN theory was unfortunately not discussed in

many of the earlier papers, including the classic paper of [3]. The limitations of the WKB approach are well known, however, in the treatment of thermionic emission; a common technique for improving the calculation[11] is to make a parabolic approximation to the top of of the barrier. Nevertheless, FN theory has been applied in regimes where it is not valid. In section 2 we shall examine the image-free problem exactly ‡, whose solution in one dimension is amenable to analytical treatment in terms of Airy type functions. Some preliminary assessment of the FN-WKB can already be made for this case, which is a preamble to the full image problem which we shall treat in section 3 by various analytical methods. Interestingly the tunnelling problem close to the barrier top appears to be amenable to analytical treatment as well and has not been published to the best of our knowledge. We shall note that the failure of the WKB criteria coincides quite closely to this regime, hence the availability of analytical results are extremely welcomed. Next we shall note that the role of screening has also been omitted in the original FN theory. We shall introduce the additional screening potentials in section 4 and thereby propose that this is one mechanism for a significant barrier reduction, in addition to negative electron affinity attributed to diamond like carbon systems. In section 5 we shall apply our theory to the analysis of experimental data for carbon field emitters[12]. Regardless of reasonable assumptions of point tip field enhancement effects, we shall see that the FN theory does not even get close to the order of magnitude agreement with the data by comparison with ours. We shall conclude in section 6 with a summary of our results, postponing further solutions of the problem involving screening to a future paper.

## 1. WKB Validity criteria

Following [10] it is straightforward to derive the criterion for the validity of WKB:

$$p^3 \gg m\hbar eF, \quad (5)$$

where  $F$  is the external field and we shall ignore the electron image for the moment. Here  $p$  is the electron momentum so that:

$$(2m(\phi - eFx))^{3/2} \gg m\hbar eF, \quad (6)$$

where  $\phi$  is the work function. Assuming a carrier effective mass equal to the free electron mass and inserting numerical values appropriate to a field in V/ $\mu\text{m}$  and a work function in eV, (which shall be our units throughout this paper) gives

$$\zeta(F, \phi) = 0.046 \frac{F^{1/3}}{(\phi)^{1/2}} \ll 1, \quad (7)$$

in which the tunnelling length  $x$  has been set to zero, representing the best case for WKB, the very top of the barrier ( $x$  is typically of the order of nm). Typical numerical values for  $\zeta$  are given table 1, where we see that the WKB approximation begins to

‡ Since image effects are less important for silicon based Schottky junctions due to the large dielectric constant  $\epsilon_s \approx 11.9$ , these results are actually very relevant to the latter, which however we shall not take up here in this paper.

**Table 1.** Values of the function  $\zeta(F, \phi)$ . For WKB theory to be valid,  $\zeta(F, \phi) \ll 1$ .

$F(\text{V}/\mu\text{m})$	$\phi = 1 \text{ eV}$	$\phi = 5 \text{ eV}$	$\phi = 10 \text{ eV}$
1	0.046	0.021	0.015
10	0.099	0.044	0.031
100	0.213	0.096	0.068
1000	0.460	0.206	0.146

be questionable for fields above about  $10\text{V}/\mu\text{m}$  for typical work function values and is certainly seriously questionable in the range close to dielectric breakdown fields which are typically  $10^3 \text{ V}/\mu\text{m}$ . A smaller effective mass such as for p-Si where ( $m^* = 0.6$  for holes) would increase  $\zeta$  further. Later on in the paper we shall show further anomalies with the FN theory when we are close to this limit of validity. In order to proceed and be able to assess the approximation further we shall have to resort to a full solution of the Schrodinger equation which we shall begin in the next section by first ignoring the image potential.

## 2. Exact solution without electron images

We shall start with the image free tunnelling problem given by the Schrodinger equation:

$$\psi''(x) + \frac{2m}{\hbar^2}[W - V(x)]\psi(x) = 0, \quad (8)$$

where  $W$  is the energy eigenvalue of the Hamiltonian  $H_0$  with the potential given by [3]:

$$V(x) = \begin{cases} -W_a & \text{if } x < 0 \text{ - region 1;} \\ V_0 - eFx & \text{if } x > 0 \text{ - region 2.} \end{cases} \quad (9)$$

Here  $V_0$  under normal circumstances is zero which yields the work function  $\phi$  as the barrier height and  $F$  is as before the applied external field. For later convenience we shall recast Eq(8) into the more compact form:

$$\psi''(x) + (\epsilon + \alpha x)\psi(x) = 0, \quad (10)$$

with

$$\begin{aligned} \alpha &= \frac{2meF}{\hbar^2} \approx F \times 2.55989 \times 10^7 (\mu\text{m})^{-3}, \\ \epsilon &= \frac{2m(W - V_0)}{\hbar^2} \approx (W - V_0) \times 2.55989 \times 10^7 (\mu\text{m})^{-2}, \end{aligned} \quad (11)$$

in which  $F$  is measured in  $\text{V}/\mu\text{m}$ . To the best of the authors' knowledge this elementary quantum exercise does not seem to have been fully documented in the literature, although variants of it have been scattered around [13, 14, 15, 16]. Following Landau

and Lifshitz [10], we shall transform to the new variable  $\xi = (x + \epsilon/\alpha)\alpha^{1/3}$ . Then equation (10) in region 2 becomes the typical Airy's equation §:

$$\psi''(\xi) + \xi\psi(\xi) = 0. \quad (12)$$

However some care needs to be exercised in selecting the appropriate type of Airy functions, since the standard Ai function has asymptotic form [10, 17]:

$$\psi(\xi) = \text{Ai}(-\xi) \approx \xi^{-1/4} \sin\left(\frac{2}{3}\xi^{3/2} + \pi/4\right). \quad (13)$$

As this also contains a reflected wave, it is not appropriate to our boundary conditions. The correct approach is to revert to the original 1/3 fractional Bessel functions definition for the Airy functions and then construct appropriate linear combinations to yield the forward travelling wave solution only. This approach of course leads to a modified appropriate Hankel function which as we shall see has the correct asymptotic form required. It is this construction that seems to be rather rarely seen in the literature except perhaps in the WKB derivation of Moll [16]. With this proviso, we can write down the solution for the wave functions of equation (12) as:

$$\psi(x) = \begin{cases} e^{ikx} + re^{-ikx} & \text{in region 1;} \\ t[u_1(\xi) - e^{-i\pi/3}u_2(\xi)] & \text{in region 2,} \end{cases} \quad (14)$$

where  $k = (2m(W + W_a)/\hbar^2)^{1/2}$  and the  $u_1$  and  $u_2$  are given by Bessel functions of order 1/3, here defined as:

$$u_1(\xi) = \frac{1}{3}(\pi\xi)^{1/2} J_{-1/3}\left(\frac{2}{3}\xi^{3/2}\right), \quad (15)$$

and

$$u_2(\xi) = \frac{1}{3}(\pi\xi)^{1/2} J_{1/3}\left(\frac{2}{3}\xi^{3/2}\right), \quad (16)$$

respectively. Note however that analytical continuation to negative  $\xi$  requires some care: see Appendix A. It is then straightforward to obtain the reflection and transmission amplitudes by matching the wave functions and their derivatives at the interface  $x = 0$ . We provide the results here in terms of  $H_{1/3} = u_1 - e^{-i\pi/3}u_2$  which is a slightly modified Hankel function

$$t = \frac{2}{H_{1/3}(\xi_0) - ik_0^{1/3}H'_{1/3}(\xi_0)}$$

$$r = \frac{H_{1/3}(\xi_0) + ik_0^{1/3}H'_{1/3}(\xi_0)}{H_{1/3}(\xi_0) - ik_0^{1/3}H'_{1/3}(\xi_0)}, \quad (17)$$

where  $\xi_0 = \xi(0) = \bar{\epsilon} = \epsilon/\alpha^{2/3}$  while  $k_0^{1/3} = \alpha^{1/3}/k$ . An important check must be made to these formulas which requires that the transmission coefficient:

$$T = \frac{k_0^{1/3}}{4}|t|^2, \quad (18)$$

§ The advantage of using the Airy function formulation is that it naturally takes care of the long range boundary condition posed by the electric field.

and reflection coefficient:  $R = |r|^2$  satisfy the unitarity property  $T + R = 1$ . This is easily checked to be the case when appropriate use is made of the Wronskian identity:

$$u_1 u_2' - u_2 u_1' = \frac{1}{2\sqrt{3}}. \quad (19)$$

For sufficiently small fields, we can obtain an asymptotic expansion (where  $\xi_0 \rightarrow \infty$  and  $k_0 \rightarrow 0$ ) that yields:

$$T_{asympt} \approx \frac{4k_0^{1/3} |\xi_0|^{1/2}}{(1 + k_0^{2/3} |\xi_0|)} e^{-\frac{4}{3}\xi_0^{3/2}}, \quad (20)$$

the prefactor being a new result not obtainable within WKB. For convenience we set  $W_a = 2\phi$  which for  $\phi$  of order 1 eV is adequate as a lower bound (at room temperatures), the exception being very narrow band semiconductors which we are not concerned with here. We shall at the moment ignore any possible barrier height lowering (i.e. image free case) so that  $V_0 = 0$  is the vacuum level and consider tunnelling near the Fermi level, so that  $W = -\phi$  and thus  $k_0^{2/3} |\xi_0| = 1$ . Then we see that the above prefactor differs from the WKB result by a mere factor of two i.e.:

$$T_{asympt} \approx 2 e^{-\frac{4}{3}\xi_0^{3/2}}. \quad (21)$$

That this asymptotic result is valid for only small fields is clearly seen now for otherwise if we naively allow the field to be large, then we could arrive at an unphysical result in which  $T > 1$  which is absurd. In fact this occurs for  $\phi = 1$  eV when  $F$  reaches the order of 9.9 kV/ $\mu$ m. Hence the use of the WKB formula for large transmissions without knowledge of the prefactor in the transmission can be dangerous. Unfortunately this caution does not seem to have been exercised by Good and Müller [3], nor by Murphy and Good [18]. The latter have derived widely used criteria [19] for the validity of FN theory on the basis of the WKB integrand properties equation (4) alone, which is thus a logically inadequate procedure. If we examine the classic FN formula for the emission current:

$$J = \frac{1.54 \times 10^2 F^2}{\phi t^2 (0.0379 \times F^{1/2} / \phi)} \exp - \left( \frac{6830 \times \phi^{3/2}}{F} v(0.0379 \times F^{1/2} / \phi) \right) \text{ A cm}^{-2} \quad (22)$$

in which  $t(x)$  and  $v(x)$  are given in terms of elliptic integrals, for  $\phi = 2$  eV say, the exponent practically vanishes at  $F \approx 3000\text{V}/\mu\text{m}$ . Hence the entire emission current comes from the supply function which is the  $F^2$  factor and, as discussed above, this can be untenable. In fact it is well known from elementary quantum mechanics that the transmission coefficient is in general not unity at the top of the barrier [20].

Later on, in section 3, we shall see that an exact solution is obtainable for the full image theory at the top of the barrier, in which the transmission coefficient has a finite value less than unity, but nevertheless with significant tunnelling current contributions. As far as we are aware, this solution has not been noted in the field emission literature for the last 40 years. In figure 1 we provide two curves that compare the exact transmission coefficient equation (18) for the image free case against the asymptotic formula equation (21) close to the Fermi level for very large fields where the latter becomes problematic.

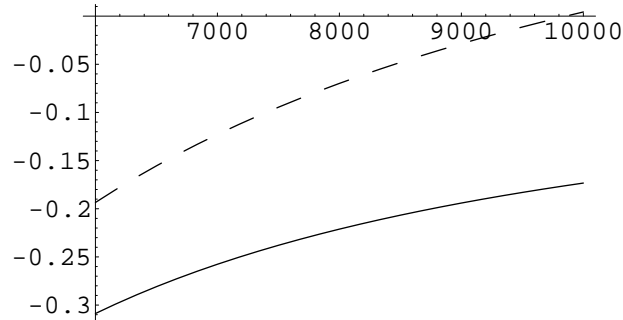


**Figure 1.** Log-linear plot of the exact transmission coefficient (solid line) equation (18) vs the asymptotic formula equation (21) (dashed line) close to the Fermi-level in the image-free case for large fields.  $F$  is in units of  $V/\mu\text{m}$ .

Fortunately these fields are very large and being much greater than typical breakdown fields this failure is unimportant in practice. We note that for smaller fields figure 2 the WKB formula is quite good, in spite of its failure to satisfy our earlier criterion of section 1. The accuracy of the WKB for small fields is however due to us staying away from the top of the barrier. We now compare equation (21) with the exact result equation (18) as we approach the barrier, i.e.  $V_0 \rightarrow -\phi$ . One mechanism for this to occur could be due to a large image term i.e. Schottky effect, but there are other screening effects as well as we shall see later. For simplicity we shall not include the image effect in the Schrodinger equation yet but merely consider the effect of approaching the barrier top in the image free case first. Here we can compare the results of three formulas, the exact equation (18), the asymptotic formula equation (20) and the standard WKB result in which the prefactor in equation (20) is missing: these are shown in figure 3, where we have set  $V_0 = -0.95 \phi$ . Here we see that for quite small fields  $F < 100V/\mu\text{m}$ , significant departures from WKB are found. These results motivate us to further include the Schottky image term in the Schrodinger equation which we take up in the next section.

### 3. Exact solution including electron images

We now turn to the quantum tunnelling problem including the effect of the image term as in the original FN theory. Then equation (10) becomes:

$$\psi''(x) + \left[ \epsilon + \alpha x + \frac{\beta}{x} \right] \psi(x) = 0, \quad (23)$$

where the image potential is characterized by the parameter  $\beta = me^2/(2\hbar^2)$ . Transforming to the parameter  $\xi$  as before we now have the equation:

$$\psi''(\xi) + \left[ \xi + \frac{\bar{\alpha}}{\xi - \bar{\epsilon}} \right] \psi(\xi) = 0, \quad (24)$$

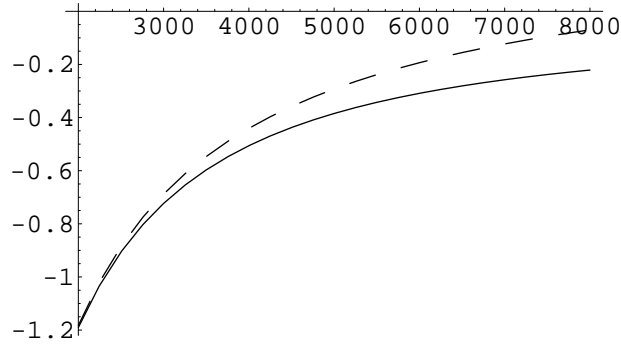


**Figure 2.** Log-linear plot of the exact transmission coefficient (solid line) equation (18) vs the asymptotic formula (dashed line) equation (21) close to the Fermi-level in the image-free case for smaller fields.  $F$  is in units of  $V/\mu\text{m}$ .

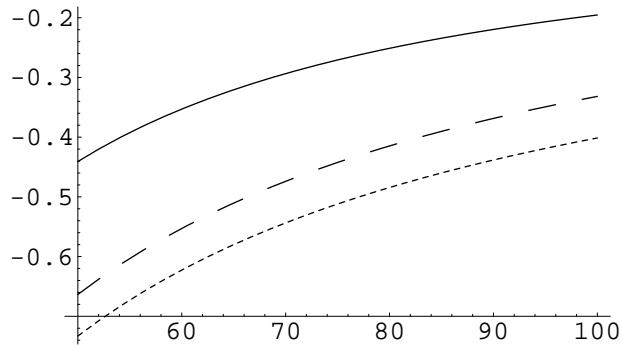


**Figure 3.** Log-linear plot of the exact transmission coefficient (solid line) equation (18) vs the asymptotic formula (dashed line) equation (20) and vs the standard WKB formula (dotted line) close to the top of the barrier ( $V_0 = -0.95 \phi$ ) in the image-free case.  $F$  is in units of  $V/\mu\text{m}$ .

where  $\bar{\alpha} = \beta\alpha^{-1/3}$ , and  $\bar{\epsilon} = \epsilon\alpha^{-2/3}$ . Clearly the image-free case  $\bar{\alpha} = 0$  reduces to the usual Airy differential equation equation (12) and the above can be rewritten as:

$$(\xi - \bar{\epsilon})\psi''(\xi) + [\xi(\xi - \bar{\epsilon}) + \bar{\alpha}]\psi(\xi) = 0. \quad (25)$$

We shall in fact further rewrite this as:

$$\psi''(\xi) + \left[ \frac{(\xi - \lambda_1)(\xi - \lambda_2)}{(\xi - \bar{\epsilon})} \right] \psi(\xi) = 0. \quad (26)$$

in which the two roots of the quadratic are given by:

$$\lambda_1 = \frac{1}{2}[\bar{\epsilon} + \sqrt{\bar{\epsilon}^2 - 4\bar{\alpha}}] \quad \text{and} \quad \lambda_2 = \frac{1}{2}[\bar{\epsilon} - \sqrt{\bar{\epsilon}^2 - 4\bar{\alpha}}]. \quad (27)$$

Let us first discuss the WKB approximation [10], which is obtained by approximating the wavefunction as:

$$\psi(\xi) = \frac{1}{\sqrt{p(\xi)}} \exp\left[i \int^\xi p(\xi') d\xi' + \frac{i\pi}{4}\right] \quad (28)$$



where:

$$p(\xi) = \left[ \frac{(\xi - \lambda_1)(\xi - \lambda_2)}{(\xi - \bar{\epsilon})} \right]^{1/2} \quad (29)$$

and the lower limit in the integral in equation (28) is the smaller of  $\lambda_1$  or  $\lambda_2$  which depends on the sign of  $\bar{\epsilon}$  i.e. above or below the barrier respectively. The evaluation of the integral in equation (28) is then a straightforward exercise in Elliptic integral reduction which we need not repeat here [2, 3, 18]. Equation (26) itself does not appear to have a closed form solution in terms of known functions although several methods of solution are available depending on the parameters. We postpone these to the appendices as we do not intend to pursue detailed calculations here, but merely to demonstrate the regimes where WKB is in need of correction. For this purpose we can concentrate on the region close to the top of the barrier at  $\xi = \bar{\alpha}^{1/2} + \bar{\epsilon}$ . Let us start at the barrier top itself for which WKB predicts  $T = 1$  since in this case  $v(x) = 0$  in equation (22). Then equation (26) simplifies to the form:

$$\psi''(\xi) + \left[ \frac{(\xi - \bar{\epsilon}/2)^2}{(\xi - \bar{\epsilon})} \right] \psi(\xi) = 0. \quad (30)$$

In view of the magnitude of the parameter  $\bar{\epsilon}$  it suffices to obtain a solution in the limit when this parameter is large. For  $\phi = 1$  eV and  $100 < F < 1000$  V/ $\mu\text{m}$ ,  $\bar{\epsilon}$  ranges from 3 to 14. In particular for the matching conditions we are only interested in the solution near to  $\xi_0 = \bar{\epsilon}$  which corresponds to the origin  $x = 0$  so that we can transform to the variable:  $y = \xi - \bar{\epsilon}$  which is small for our purpose  $y \ll \bar{\epsilon}$  so that equation (30) can be approximated by:

$$y\psi''(y) + (y + \bar{\epsilon}/2)^2\psi(y) \approx y\psi''(y) + (\bar{\epsilon}/2)^2\psi(y) = 0. \quad (31)$$

The appropriate solution for the above is then given by the Hankel function of order 1 which upon transforming back to the original variables  $\xi$  is given by:

$$\psi(\xi) = e^{i\pi/4} \sqrt{\frac{\pi}{2}} \bar{\epsilon}(\xi - \bar{\epsilon})^{1/2} H_1^{(1)}(\bar{\epsilon}(\xi - \bar{\epsilon})^{1/2}). \quad (32)$$

We can now obtain the transmission coefficient as was done in the previous section by matching the wave function and its derivative at the origin. The result is now given by:

$$T = \frac{2\bar{\epsilon}^2 k_0^{1/3}}{|\psi(\xi_0)|^2 + \epsilon^2 k_0^{1/3} + k_0^{2/3} |\psi'(\xi_0)|^2} \quad (33)$$

where the derivative of  $\psi$  is easily shown to be given in terms of the Hankel function of order 0:

$$\psi'(\xi) = e^{i\pi/4} \sqrt{\frac{\pi}{8}} \bar{\epsilon}^2 H_0^{(1)}(\bar{\epsilon}(\xi - \bar{\epsilon})^{1/2}) \quad (34)$$

As usual we can verify that this solution satisfies unitarity  $T + R = 1$  through the use of the appropriate Wronskian identities for the Hankel functions. That this is satisfied exactly in spite of our approximation in equation (31) means that we have picked out the essential features in the theory. Equation (33) gives zero transmission at the top of

the barrier because of a weak logarithmic singularity (typical of the  $1/x$  potential near the origin) in  $\psi'$ . We may write

$$T \approx \frac{4\pi}{\bar{\epsilon}^{3/2}(\ln(\delta^{1/2}\bar{\epsilon}))^2} \quad (35)$$

where  $\delta$  is a renormalization constant, which we can arbitrarily set to  $\delta \ll \bar{\epsilon}$ . Physically, we may think of this as correcting for the situation in which the electron and the image charge are both at the interface by limiting the distance of closest approach to atomic dimensions. Equation (35) corrects for the error made by the WKB approximation at the top of the barrier. As a convenient choice of  $\delta$ , we require that it is chosen to limit the closest approach to the origin as  $x = a = 1\text{\AA} \parallel$  so that by the definition of  $\xi$ :

$$\delta = \frac{10^{-4}F}{\phi}. \quad (36)$$

Before proceeding further we shall briefly mention the results when we move slightly away from the top of the barrier. In this case the two roots become:

$$\lambda_1 \approx \frac{\bar{\epsilon}}{2}(1 + \sigma) \quad \text{and} \quad \lambda_2 \approx \frac{\bar{\epsilon}}{2}(1 - \sigma) \quad (37)$$

where  $\sigma = (1 - 4\bar{\alpha}/\bar{\epsilon}^2)^{1/2}$  and in the limit  $\bar{\epsilon}$  large reduces equation (31) to:

$$y\psi''(y) + \gamma^2\psi(y) = 0. \quad (38)$$

where  $\gamma = \frac{1}{2}\bar{\epsilon}(1 - \sigma^2)^{1/2}$ . This poses no difficulties and the method outlined above can be adapted to the solution. We summarize the appropriate formulas without further ado:

$$T = \frac{8\bar{\gamma}^2 k_0^{1/3}}{|\psi(\xi_0)|^2 + 4\gamma^2 k_0^{1/3} + k_0^{2/3} |\psi'(\xi_0)|^2} \quad (39)$$

where:

$$\psi(\xi) = e^{i\pi/4} \sqrt{\frac{\pi}{2}} \quad 2\gamma(\xi - \bar{\epsilon})^{1/2} H_1^{(1)}(2\gamma(\xi - \bar{\epsilon})^{1/2}) \quad (40)$$

and

$$\psi'(\xi) = e^{i\pi/4} \sqrt{\frac{\pi}{8}} \quad (2\gamma)^2 H_0^{(1)}(2\gamma(\xi - \bar{\epsilon})^{1/2}) \quad (41)$$

In figure 4 we compare the transmission coefficient equation (33) versus the FN formula equation (22) less the prefactors. We see that the FN formula is not only in error as we trespass the barrier giving a non physical value of  $T > 1$ , for the region near the top of the barrier (around  $F = 700\text{V}/\mu\text{m}$  here), it drops exponentially fast as opposed to the exact solution.

Using equation (39) we can estimate the current near the barrier top which occurs for  $F \approx 700 \text{ V}/\mu$  in this case, remembering that we have considered  $\phi=1 \text{ eV}$  and

$\parallel$  By way of comparison, the typical tunnelling length  $\zeta = \frac{\phi}{eF}$  falls in the range of  $10^4\text{\AA}$  to  $10\text{\AA}$  for  $1 < F < 10^3 \text{ V}/\mu\text{m}$ .

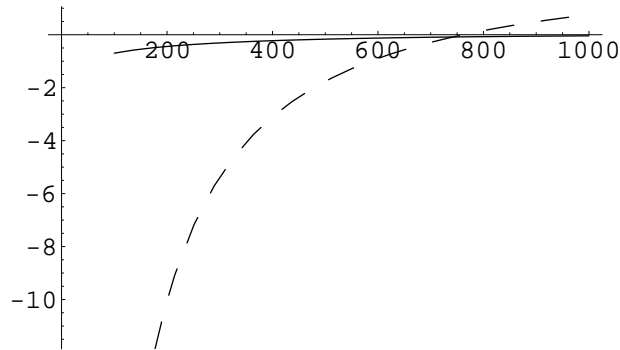


**Figure 4.** Log-linear plot of the exact transmission coefficient equation (33)(solid line) vs the FN formula (dashed line) i.e. equation (22) less the prefactors in the full image case.  $F$  is in units of  $V/\mu m$ .

$W_a = 2\phi$ . Hence for temperatures much less than  $\epsilon_F/k_B$ , the current is obtained from the integral:

$$J = \frac{4\pi me}{h^3} \int_{-W_a}^{\epsilon_F} T(W)(\epsilon_F - W)dW \quad (42)$$

which has to be evaluated numerically. We can however make an estimate using the approximate expression equation (35). We can set the Fermi level at the top of the barrier and integrate only over a small region of order  $\delta$  near to it, since outside this region the contributions are exponentially small. We choose  $\delta$  according to equation (36) as before and thus the  $\bar{\epsilon}^{-3/2}$  pre-factor dominates in the transmission coefficient since the logarithmic term is slowly varying in the region of integration. As we take  $W_a/\phi = 2$  which is large compared with  $\delta$ , we now arrive at the expression for the current density as:

$$J \approx 0.1674 \phi^{-3/2} F^3 \quad \text{A cm}^{-2} \quad (43)$$

Note that the field dependence of the current is in this case  $F^3$  which differs from the FN prediction of  $F^2$  and could be experimentally discernable in view of its non-exponential dependence. We can now compare equation (43) with the standard FN formula equation (22) see figure 5.

Having shown that we can have a large (non-exponential) current in spite of a smaller field than in the image-free case, due to proximity to the barrier top, we shall next examine other mechanisms by which the barrier lowering can occur, whose magnitude is comparable with, or might exceed the Schottky image effect. The effect to consider is due to the dielectric screening of the applied field  $F$  which we shall take up next.

#### 4. The Effects of Screening

Screening is an important property of metals or dielectrics, and the mechanism itself plays a crucial role in the previous section in the form of the image potential which is

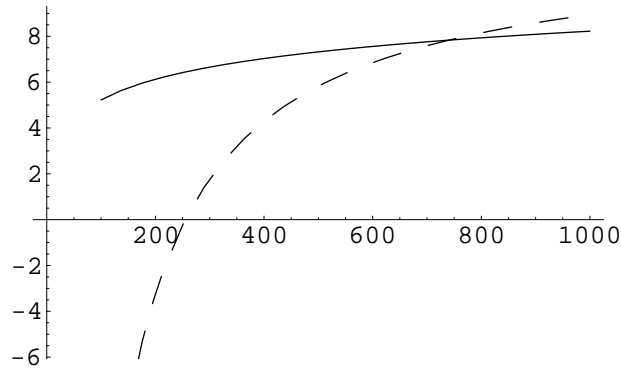


**Figure 5.** Log-linear plot of the tunnelling current near the top of the barrier (which occurs for fields of order  $700 \text{ V}/\mu\text{m}$  here) (solid line) equation (43) compared with the standard FN formula (dashed line) close to the top of the barrier in the full image case equation (22).  $F$  is in units of  $\text{V}/\mu\text{m}$ .

a screening effect. In recent years there has been a revival of interest in screening, [21] especially in semiconductors, where surface effects can significantly alter the properties of devices. On the surface the screening length, typically of the order of  $\lambda_{TF}$  from Thomas-Fermi theory ranges between the order of a few  $\text{\AA}$  for metals to a few  $\mu\text{m}$  for semiconductors or even higher to tenths of mm due to surface effects since it is the charge carrier density at the surface layer that matters. The (Laplace) screening problem for a flat surface is easily solved for an external field  $F$ . This modifies the external potential  $V(x)$  in equation (9) by having a non-zero  $V_0$  such that  $V_0 = -\lambda_{TF}eF$ . We shall neglect an exponential penetration field inside which in fact modifies the inner potential to

$$\begin{aligned} V(x) &= -W_a - \lambda_{TF}eFe^{x/\lambda_{TF}} \quad \text{for } x < 0 - \text{region 1} \\ &= -\lambda_{TF}eF - eFx \quad \text{for } x > 0 - \text{region 2} \end{aligned} \quad (44)$$

The latter leads to a 2D electron gas which requires a self-consistent theory to treat since this in turn affects our  $\lambda_{TF}$  as already mentioned. Further the proper inclusion of screening must now include its effects on the image potentials which pick up Yukawa type terms. It suffices here to estimate the barrier lowering from our expression for  $V_0$ . Since  $F$  is in  $\text{V}/\mu\text{m}$  then a  $\lambda_{TF} \approx 1 \mu\text{m}$  will completely wipe out a barrier of 1 eV. For 3D this corresponds to a carrier density of order  $10^{25} \text{ m}^{-3}$  but for a 2D layer this can be down by a 2/3 power i.e.  $10^{17} \text{ m}^{-2}$ . If we include the effects due to a diminished electron affinity as in the case of diamond-like carbon bonds, then we see that the present theory provides a strong candidate as an explanation for the high current densities in carbon granular samples recently observed in materials for field emission displays [4], as we shall see in the next section.

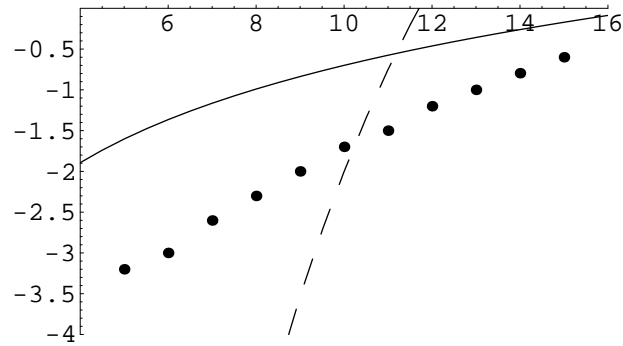


**Figure 6.** Log-linear plot of the tunnelling current vs electric field  $F$ , assuming that a significant barrier lowering mechanism ( $V_0 = 0.7\phi$ ), such as dielectric screening (see text) has occurred. The solid line is our theory, the dots are experimental points from Tuck et al [12] while the FN theory is given by the dash line. In addition a large field enhancement factor  $\gamma = 10$  has to be assumed for the FN formula equation (22). Our result compares much more favourably with the experimental points than does the FN theory.

## 5. Relation to Experiments

Comparison with experiments such as for carbon field emitters [12] can be made by assuming that there is a barrier lowering mechanism such as the dielectric screening as mentioned above. The tunnelling current will then be assumed to be given by equation (43) but we shall include a factor  $\sigma$  to account for granularity or inefficient screening (and hence barrier lowering) which diminishes the current. This modifies equation (43) trivially to:

$$J \approx 0.1674 \phi^{-3/2} \sigma^3 F^3 \quad \text{A cm}^{-2} \quad (45)$$

In figure 6 we have plotted the results which shows that for a granularity factor of  $\sigma = 0.15$  our results compare favorably with experiments [12] bearing in mind that our results are only estimates and not accurate numerical evaluations¶. In particular the parameters as given in the figures have not been fine tuned in anyway. On the contrary without assuming a significant field enhancement due to pointed tips, the FN theory is out by numerous orders of magnitude. However even with the assumption of a large field enhancement factor  $\gamma = 10$  which is reasonable for ellipsoids [23], and a barrier lowering  $V_0 = -0.7\phi$ , the FN curve figure 6 does not in any way resemble the experimental data, a feature we have found to occur quite commonly in analyzing data from the carbon field emitting samples. Note the vast order of magnitude differences and the fast drop in the slope of the FN curve which is shown more clearly in the inset to figure 6. These results clearly show that our theory has captured some essential physics associated to tunnelling near the barrier top which may be relevant to the carbon field emitters.

¶ Finite temperature effects should also be included in a more accurate calculation, providing essential improvements to thermionic field emission theory[18, 19].

## 6. Conclusion

In conclusion we have presented a closer look at the traditional FN theory of field emission and found that the latter is untenable for calculations of emission currents when significant barrier lowering occurs. A full quantum mechanical solution of the problem provides us with an estimate which, coupled with a proposed barrier lowering due to screening or negative electron affinity, constitutes a reasonable order of magnitude estimate for the high current densities in samples with embedded particles, not available via FN theory. Further work is necessary to provide more quantitative comparisons noting that the granularity of the systems would lead to less total current density although on the other hand some field enhancements due to shape effects [22, 23] not considered here might partially compensate for this loss.

## Acknowledgements

We wish to acknowledge the support of the Engineering and Physical Sciences Research Council through grants GR/M71404/01 and GR/R97047/01.

## 7. References

- [1] Fowler R H and Nordheim L W (1928) *Proc. R. Soc. Lond.* **A119**, 173-181.
- [2] Nordheim L W (1928) *Proc. R. Soc. Lond.* **A121**, 626-639.
- [3] Good R H and Müller E W (1956) in *Handbuch der Physik*, edited by S. Flugge, (Springer, Berlin) vol XXI, pp 176-191.
- [4] Burden A P (2001) Materials for field emission displays, *International Materials Reviews* **46**, 213-231.
- [5] Sze S M (1981) *Physics of Semiconductors*, second edition *John Wiley and Sons*, 254-265 and references quoted therein.
- [6] Mott N F and Gurney R W (1948) *Electronic Processes in Ionic Crystals* (OUP).
- [7] Herring C H (1950) *Rev. Mod. Phys.* **21**, 187.
- [8] Dearnaley G, Stoneham A M and Morgan D V (1970) *Rep. Prog. Phys.* **33**, 1129.
- [9] Good R H and Miller S C Jr (1953) *Phys. Rev.* **91**, 174-182.
- [10] Landau L D and Lifshitz E M (1991) *Quantum Mechanics* (Pergamon) p 165.
- [11] Guth E and Mullin C J (1940) *Phys. Rev.* **59**, 575.
- [12] Tuck R A et al (1997) *Proceedings of the Fourth IDW* 723-726.
- [13] Roy D K (1977) *Tunnelling and negative resistance phenomena in semiconductors*, International Series in the Science of the Solid State (Pergamon) vol 11, p 53.
- [14] Delbourgo R (1977) *Am. J. Phys.* **45**, 1110-1112.
- [15] Duke C B (1969) *Tunnelling in Solids*, Supplement 10 to Solid State Physics, edited by F Seitz, D Turnbull and H Ehrenreich (Academic Press).
- [16] Moll J L (1964) *Physics of Semiconductors*, (McGraw-Hill).
- [17] Watson G H (1944) *Theory of Bessel Functions* (CUP) 77.
- [18] Murphy E L and Good R H Jr (1956) *Phys. Rev.* **102**(6), 1464-1473.
- [19] Stratton R (1962) *Phys. Rev.* **125**(1), 67-82.
- [20] Schiff L I (1965) *Quantum Mechanics* (McGraw Hill) p103.
- [21] Choy T C (2000) *Image charges revisited: a closed form solution*, Los Alamos National Laboratory archive <http://xxx.lanl.gov/cond-mat/0011092> and references therein.

[22] —(1999) *Effective Medium Theory- Principles and Applications* (OUP) 7-15 and references therein.

[23] Jaeger D L, Hren J J and Zhirnov V V (2003) *J. Appl. Phys* **93**(1), 691-697.

## Appendix A. Analytical continuation of Bessel Functions

Confusion arises with Bessel functions of order  $1/3$  due to special care needed to treat the phase factors: some popular mathematical software uses incorrect continuation formulae. Firstly our convention is the same as Watson's so that the appropriate continuation formula is given by:

$$I_\nu(z) = \begin{cases} e^{-i\nu\pi/2} J_\nu(ze^{i\pi/2}) & \text{if } -\pi < \arg(z) \leq \pi/2 \\ e^{3i\nu\pi/2} J_\nu(ze^{-3i\pi/2}) & \text{if } \pi/2 < \arg(z) \leq \pi. \end{cases} \quad (\text{A.1})$$

An alternative approach is to perform the continuation for negative  $z$  as:

$$\begin{aligned} u_1 &= \frac{\sqrt{\pi} \sqrt{x} J_{-1/3}(\frac{2}{3} x^{\frac{3}{2}})}{3} = \frac{i}{3} \sqrt{\pi} \sqrt{|x|} J_{-1/3}(\frac{-2i}{3} |x|^{\frac{3}{2}}) \\ &= \frac{i}{3} e^{i\pi/6} \sqrt{\pi} \sqrt{|x|} I_{-1/3}(\frac{2}{3} |x|^{\frac{3}{2}}), \end{aligned} \quad (\text{A.2})$$

which is incorrect. The negative argument prevents the use of the first form of equation(A.1). Instead the branch cut properties requires the continuation formula [17]:

$$J_\nu(e^{im\pi/2} z) = e^{im\pi/2} J_\nu(z) \quad (\text{A.3})$$

which holds similarly for the  $I_\nu$  functions. Then:

$$u_1 = \frac{\sqrt{\pi} \sqrt{x} J_{-1/3}(\frac{2}{3} x^{\frac{3}{2}})}{3} = \frac{i}{3} \sqrt{\pi} \sqrt{|x|} J_{-1/3}(\frac{-2i}{3} |x|^{\frac{3}{2}}) = \frac{1}{3} \sqrt{\pi} \sqrt{|x|} I_{-1/3}(\frac{2}{3} |x|^{\frac{3}{2}}), \quad (\text{A.4})$$

without any complex phase factors. Similarly  $u_2$  picks up a minus sign:

$$u_2 = \frac{\sqrt{\pi} \sqrt{x} J_{1/3}(\frac{2}{3} x^{\frac{3}{2}})}{3} = \frac{i}{3} \sqrt{\pi} \sqrt{|x|} J_{1/3}(\frac{-2i}{3} |x|^{\frac{3}{2}}) = \frac{1}{3} - \sqrt{\pi} \sqrt{|x|} I_{1/3}(\frac{2}{3} |x|^{\frac{3}{2}}). \quad (\text{A.5})$$

Hence one has to manually continue the  $J_\nu$  to the  $I_\nu$  functions for negative arguments when if using the incorrect continuation, equation (A.2). We have found that Mathematica v4.1 uses equation (A.2).

## Appendix B. Power series solution for the full image problem I

The generic form of the full image problem is given by the following second order differential equation

$$\psi'' + \left( \epsilon + \alpha x + \frac{\beta}{x} \right) \psi = 0. \quad (\text{B.1})$$

As before a straightforward linear transformation:  $\xi = (x + \frac{\epsilon}{\alpha})\alpha^{\frac{1}{3}}$  leads to the following form:

$$\psi'' + \xi \psi + \frac{\bar{\alpha}}{\xi - \bar{\epsilon}} \psi = 0, \quad (\text{B.2})$$

where  $\bar{\alpha} = \beta\alpha^{-\frac{1}{3}}$ , and  $\bar{\epsilon} = \epsilon\alpha^{-2/3}$ . Clearly the image free case  $\bar{\alpha} = 0$  reduces to the usual Airy differential equation. Equation (B.2) can be rewritten as:

$$(\xi - \bar{\epsilon})\psi'' + \xi(\xi - \bar{\epsilon})\psi + \bar{\alpha}\psi = 0. \quad (\text{B.3})$$

Unfortunately this equation does not belong to the standard hypergeometric class and cannot therefore be treated by the usual mathematical physics functions. However using the standard Frobenius method one can obtain the following power series solutions. Let

$$u_m(\xi) = \sum_{n=0}^{\infty} a_n \xi^{m+n}, \quad (\text{B.4})$$

then equation (B.4) leads to the following 5 term recursion relation for the determination of the coefficients  $a_n$ :

$$\begin{aligned} a_{n-1}(m+n-1)(m+n-2) - a_n\bar{\epsilon}(m+n)(m+n-1) \\ + a_{n-4} - \bar{\epsilon}a_{n-3} + \bar{\alpha}a_{n-2} = 0. \end{aligned} \quad (\text{B.5})$$

All the coefficients are well determined in terms of the coefficient  $a_0$ . The first term satisfies

$$\bar{\epsilon}m(m-1)a_0 = 0, \quad (\text{B.6})$$

giving  $m = 0$  or  $m = 1$  which shows as expected that we shall have two linearly independent solutions. Carrying on we have  $a_1 = 0$  and

$$a_2 = \frac{\bar{\alpha}}{\bar{\epsilon}} \frac{a_0}{(m+2)(m+1)}. \quad (\text{B.7})$$

Notice that  $a_1 = 0$  regardless but  $a_2$  is only finite for  $\bar{\alpha} \neq 0$ , i.e.  $\beta \neq 0$ . The following coefficients can be sequentially determined:

$$a_3 = \frac{a_2(m+1)}{\bar{\epsilon}(m+3)} - \frac{a_0}{(m+3)(m+2)}, \quad (\text{B.8})$$

$$a_4 = \frac{a_3(m+2)}{\bar{\epsilon}(m+4)} + \frac{a_0}{\bar{\epsilon}(m+4)(m+3)} + \frac{\bar{\alpha}}{\bar{\epsilon}} \frac{a_2}{(m+4)(m+3)}, \quad (\text{B.9})$$

and so on. The general 5 term recursion relation can be re-written as

$$\begin{aligned} a_n = \frac{1}{(m+n)(m+n-1)} \\ \left[ \frac{1}{\bar{\epsilon}} a_{n-1}(m+n-1)(m+n-2) + \frac{\bar{\alpha}}{\bar{\epsilon}} a_{n-2} - a_{n-3} + \frac{1}{\bar{\epsilon}} a_{n-4} \right]. \end{aligned} \quad (\text{B.10})$$

Unfortunately there is no way to simplify this any further. When  $\bar{\alpha} = 0$  (image free case) the above in fact reduces to a two term relation given by:

$$a_n = -\frac{a_{n-3}}{(m+n)(m+n-1)}. \quad (\text{B.11})$$

This immediately leads us to the two independent solutions, for  $m = 0$

$$\begin{aligned} u_0(\xi) &= 1 + \sum_{n=1}^{\infty} \frac{(-1)^n 1.4.7 \dots (3n-2)}{(3n)!} \xi^{3n} \\ &= \frac{\Gamma(2/3)}{3^{1/3}} \xi^{1/2} J_{-1/3}\left(\frac{2}{3}\xi^{3/2}\right), \end{aligned} \quad (\text{B.12})$$



and for  $m = 1$

$$\begin{aligned} u_1(\xi) &= \xi + \sum_{n=1}^{\infty} \frac{(-1)^n 2.5.8 \dots (3n-1)}{(3n+1)!} \xi^{3n+1} \\ &= 3^{1/3} \Gamma(4/3) \xi^{1/2} J_{1/3} \left( \frac{2}{3} \xi^{3/2} \right), \end{aligned} \quad (\text{B.13})$$

which are the series expansions for the Bessel functions of order  $1/3$ . The oscillatory nature of these functions means that the convergence is in general poor and some more sophisticated re-summation method must be used to obtain in particular the asymptotic properties of these functions. In the next appendix we shall show just one method as to how this can be achieved.

### Appendix C. Power series solution for the full image problem II

An alternative solution for the full image problem which is an effective re-summation of the previous power series solution that will allow us to perform numerical calculations, will now be shown. The approach is to first use a Laplace transform on equation (B.1). Let

$$\psi(\xi) = \int_C e^{\xi t} f(t) dt, \quad (\text{C.1})$$

over some contour  $C$ , then the resulting differential equation in  $\psi$  becomes converted into a second-order differential equation in  $f$ :

$$f'' - (t^2 - \bar{\epsilon})f' + (\bar{\alpha} - \bar{\epsilon} t^2 - 2t)f = 0. \quad (\text{C.2})$$

It is easy to show that the solution for  $\bar{\alpha} = 0$  reduces to the Airy integral where  $f(t) = e^{t^3/3}$  so we shall factorize  $f$  in the form:  $f = ug$  where  $u = e^{t^3/3}$ . The equation for  $g$  now simplifies tremendously:

$$g'' + (t^2 + \bar{\epsilon})g' + \bar{\alpha}g = 0. \quad (\text{C.3})$$

Unfortunately there is still no closed form solution for this equation although it can be proved that solutions for  $g$  must be an entire function, by which we can develop an expansion as an infinite series:

$$g = \sum_{n=0}^{\infty} a_n t^{m+n}. \quad (\text{C.4})$$

The boundary condition requires that when  $\bar{\alpha} \rightarrow 0$  then  $g \rightarrow 1$ . With this we can show that  $m = 0$  is the only allowed index. Then we have the following 4 term recursion relation:

$$(n-1)(na_n + \bar{\epsilon}a_{n-1}) + (n-3)a_{n-3} + \bar{\alpha}a_{n-2} = 0. \quad (\text{C.5})$$

The first few solutions are easily obtained:  $a_0 = 1$ ,  $a_2 = \frac{\bar{\alpha}}{2}$ ,  $a_3 = \frac{\bar{\epsilon}\bar{\alpha}}{6}$ ,  $a_4 = \frac{\bar{\alpha}}{24}(\bar{\alpha} - \bar{\epsilon}^2)$  and so on. As required only the first term survives in the limit  $\bar{\alpha} = 0$ . Interestingly the 4 term relation equation (C.5) can actually be reduced to a three term one. Let  $\gamma_n = \frac{a_n}{a_{n-1}}$  then

$$(n-1)(n\gamma_n + \bar{\epsilon})\gamma_{n-1} + \frac{(n-3)}{\gamma_{n-2}} + \bar{\alpha} = 0, \quad (\text{C.6})$$

which may be more convenient for computation. Finally we have now effectively re-summed the series to obtain

$$\psi(\xi) = \sum_{n=0}^{\infty} a_n \int_C t^n e^{\xi t + \frac{1}{3}t^3} dt. \quad (\text{C.7})$$

We now see that

$$\begin{aligned} \int_C t^n e^{\xi t + \frac{1}{3}t^3} dt &= \frac{d^n}{d\xi^n} \int_C e^{\xi t + \frac{1}{3}t^3} dt \\ &= \frac{d^n}{d\xi^n} \left[ \xi^{1/2} Z_{\pm 1/3} \left( \frac{2}{3} \xi^{3/2} \right) \right], \end{aligned} \quad (\text{C.8})$$

the last term following from the equivalence between the Airy functions and the Bessel functions of order  $1/3$ . In view of the recursion properties for the derivatives of the Bessel functions, we have now converted the solution effectively into an infinite series of Bessel functions. Only the first term survives in the image free case which is now trivial and all the oscillatory bits are now absorbed into the Bessel functions.